resents Eq. (6) or its equivalent; $\eta(C)$; and $\alpha_{W,\,max}$, an equation which estimates, at each solution, the value of α_W which will produce zero net mass fraction. The search variables are generally μ_W, T_H (heliocentric trip time), T_D (departure trip time), V_∞, and r_1 (radius of impulsive thrust application). Figure 2 presents a typical set of results.

Some General Considerations

As experienced here, the following items have major effects on the structure and formulation of the model: 1) purpose of the model, 2) level of detail required, 3) number of flight profiles and system variations, 4) the submodels available, and 5) the choice of optimization techniques.

Generally, it is advantageous in terms of machine time and convergence to employ approximations for the trajectory requirements in the different flight modes. Further, approximation techniques for representing the interrelationship between the trajectory and the vehicle are useful in permitting separate and distinct subroutines for each.

If the numerical procedure or, in fact, the solution of any set of equations within the model requires an iterative procedure with input starting guesses, it is most efficient to specify a system parameter (e.g., α_W) as the principle variable for a given set of system and flight conditions. In this way starting solutions for both search variables and other parameters are generated internally, and information will be available for various α_W's should the particular desired α_W (or some lower value) encounter nonconvergence or yield unacceptable net mass fractions.

A task which merits intensive analysis is the inclusion of a probabilistic characterization of the electric propulsion system's probable degradation with time due to component failure. Computer programs are needed for optimizing heliocentric, power-limited, constant-thrust trajectories with power output varying, preferably, as a function of both time and position. Reference 8 includes an initial attempt at introducing power system reliability aspects into mission studies.

A compilation of the known low-thrust system and flight mode concepts should be made in order to develop a common basis of comparison for the many studies and mission models yet to come.

References

[1] Van Dine, C. P., "Extension of the Finite-Difference Newton-Raphson Algorithm to the Simultaneous Optimization of Trajectories and Associated Parameters," AIAA Paper 68-115, New York, 1968.

[2] Ragsac, R. V., "Trajectory Requirements and Performance Computations of Single-Stage Electrically Propelled Space Vehicles," Paper 68-106, 1968, AAS.

[3] Hooke, R. and Jeeves, T. A., "Direct Search Solution of Numerical and Statistical Problems," *Journal of the Association of Computing Machinery*, Vol. 8, 1961, pp. 212–223.

[4] Johnson, F. T., "Approximate Finite-Thrust Trajectory Optimization," Paper 68-080, 1968, AAS.

[5] Fimple, W. R. and Edelbaum, T. N., "Applications of SNAP-50 Class Power-plants to Selected Unmanned Electric Propulsion Missions," AIAA Paper 64-194, Wichita, Kansas, 1964.

[6] Melbourne, W. G. and Sauer, C. G., Jr., "Performance Computations with Pieced Solutions of Planetocentric and Heliocentric Trajectories for Low-Thrust Missions," *Jet Propulsion Laboratory Space Programs Summary No. 37–36*, Vol. IV, Pasadena, Calif., 1965.

[7] Melbourne, W. G. and Sauer, C. G., "Payload Optimization for Power-Limited Vehicles," *Progress in Astronautics and Aeronautics: Electric Propulsion Development*, Vol. 9, edited by E. Stuhlinger, Academic Press, New York, 1962, pp. 617–645.

[8] Gitlow, B., Schmitt, J. W., and Ragsac, R. V., "Rankine Cycle Powerplant Characteristics for Electric Propulsion Manned Mars Mission," AIAA Paper 66-894, Boston, Mass., 1966.

Dimensionless Products of Parachute Inflation

Kenneth E. French*
Lockheed Missiles & Space Company, Sunnyvale, Calif.

Nomenclature

- D_0 = parachute constructed diameter, m or ft
- F_0 = parachute opening shock, N or lb
- f_i = symbol denoting functional relationship ($i = 1,2$)
- g = acceleration of gravity, m/sec² or ft/sec²
- M = total system mass, kg or slug
- q_s = dynamic pressure at time of full line stretch, N/m² or lb/ft²
- S_0 = parachute reference drag area, m² or ft² ($= \frac{1}{4}\pi D_0^2$)
- t_f = parachute inflation time, sec
- v_s = system velocity at time of full line stretch, m/sec or ft/sec
- θ = average flight-path angle during inflation, deg or rad
- ρ = atmosphere mass density, kg/m³ or slug/ft³

Introduction

As noted previously,[1,2] dimensional considerations indicate that incompressible-flow parachute inflation may be characterized by the dimensionless products

$$F_0/q_sS_0 = f_1[(\rho D_0^3/M),\ (gD_0 \sin\theta/v_s^2)] \tag{1}$$

and

$$v_st_f/D_0 = f_2[(\rho D_0^3/M),\ (gD_0 \sin\theta/v_s^2)] \tag{2}$$

In Eqs. (1) and (2), F_0 and t_f are the variables of interest. Methods or formulas are available for the calculation of t_f for some types of parachute. These methods encompass the "infinite mass" case,[3,4] in which system velocity remains constant during inflation, and certain ranges of test conditions.[5] Methods are also available for calculation of F_0, but are rather cumbersome to apply. None of the available methods indicate the tolerances to be expected in the calculated variable under actual flight test conditions.

Equations (1) and (2) suggest that an appreciation of the dispersion to be encountered in the parachute inflation process could be obtained by plotting F_0/q_sS_0 vs v_st_f/D_0 from test data. Such a plot would also provide a useful cross-check on (or short-cut to) methods that calculate F_0 based on an initial calculation of t_f.

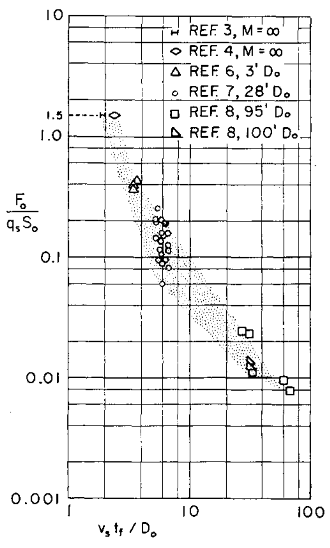

Fig. 1 F_0/q_sS_0 vs v_st_f/D_0 for various parachutes.

Received July 14, 1969.

* Staff Engineer. Associate Fellow AIAA.

Table 1 Summary of parachute test data

Parachute		Range of test conditions		
Type	Geometry	v_s, fps	q_s, lb/ft²	Ref.
Flat circular	3-ft D_0, 28-gore	50–85	3–8.5	6
Flat circular	28-ft D_0, 28-gore	154–288	18.6–50.6	7[a]
Flat circular	100-ft D_0, 120-gore, single-reefed stage	263–324	76–116	8
Conical	95-ft D_0, 108-gore, single-reefed stage	218–454	53–227	8

[a] Four tests reported by Berndt in which the chute squidded at $v_s >$ 300 fps are omitted.

Test Data

Figure 1 shows the suggested plot of F_0/q_sS_0 vs v_st_f/D_0. In the figure, the values of v_st_f/D_0 at $F_0/q_sS_0 = 1.5$ correspond to the infinite mass case and were calculated from infinite mass filling time formulas for solid, flat circular chutes[3,4] with assumed effective porosity values of 0.03–0.05. The remaining points in the figure are from the test data summarized in Table 1. As noted, the 95-ft and 100-ft D_0 chutes were used with reefing, so there is some doubt if data for these chutes are really suited to comparison with unreefed chute data. However, for very large chutes reefing appears to assist symmetry of inflation more than it affects opening load or time. In addition, only those 95-ft and 100-ft D_0 chute tests in which opening force upon inflation to full blossom was greater than opening force upon inflation to reefed stage were used for Fig. 1.

Discussion

The data of Fig. 1 confirm that the parachute inflation process is subject to relatively large dispersion, yet remain well ordered enough to be amenable to empirical curve-fitting techniques. That is, if a satisfactory method can be found for calculation of t_f, data as in Fig. 1 will permit the empirical calculation of F_0 and its tolerances for the given value of t_f.

In this Note, only test data with good reporting of test variables were used. However, earlier test data on 24-ft D_0 solid, flat circular chutes have been examined and found to exhibit the same trend as in Fig. 1, although with larger scatter. Data summarized by Walcott[9] on 35, 56, and 64-ft D_0 10% extended-skirt-type parachutes likewise show the same trend as Fig. 1, but with a lower value of F_0/q_sS_0 for a given value of v_st_f/D_0, as would be expected.

It appears that useful information on the parachute opening process and its statistics can be obtained by plotting F_0/q_sS_0 vs v_st_f/D_0 for various types of parachute and by correlating the resulting data with empirical curve-fitting techniques. Figure 1 shows that some additional test data for solid, flat circular parachutes are desirable in the ranges $1.5 > F_0/q_sS_0 > 0.45$ and $0.08 > F_0/q_sS_0 > 0.025$. Test conditions required to obtain such data can be established on the basis of available scaling laws.[1]

References

[1] French, K. E., "Model Law for Parachute Opening Shock," *AIAA Journal*, Vol. 1, No. 11, Nov. 1963, pp. 2226–2228.

[2] French, K. E., "Comment on 'A Method for Calculating Parachute Opening Forces for General Deployment Conditions,'" *Journal of Spacecraft and Rockets*, Vol. 4, No. 10, Oct. 1967, pp. 1407–1408.

[3] "Performance of and Design Criteria for Deployable Aerodynamic Decelerators," ASD-TR-61-579, Dec. 1963, Flight Dynamics Lab., Wright-Patterson Air Force Base, Ohio, p. 163.

[4] Heinrich, H. G., "Opening Time of Parachutes Under Infinite Mass Conditions," *Journal of Aircraft*, Vol. 6, No. 3, May–June 1969, pp. 268–272.

[5] Berndt, R. J. and DeWeese, J. H., "Filling Time Prediction Approach for Solid Cloth Type Parachute Canopies," *Proceedings of the 1st Aerodynamic Decelerator Systems Conference*, AIAA, New York, 1966, pp. 17–32.

[6] Heinrich, H. G. and Noreen, R. A., "Analysis of Parachute Opening Dynamics with Supporting Wind Tunnel Experiments," AIAA Paper 68-924, El Centro, Calif., 1968.

[7] Berndt, R. J., "Experimental Determination of Parameters for the Calculation of Parachute Filling Times," *Jahrbuch 1964 der WGLR*, Vieweg und Sohn, Braunschweig, Germany, 1965, Table 1, p. 305.

[8] Gimalouski, E. A., "Development of a Final Stage Recovery System for a 10,000 Pound Weight," WADC TR 59-109, Dec. 1958, Wright-Patterson Air Force Base, Ohio.

[9] Walcott, W. B., "Study of Parachute Scale Effects," ASD-TDR-62-1023, Jan. 1963, Air Force Systems Command, Wright-Patterson Air Force Base, Ohio.

Evaluation of a Quartz-Fiberfrax Heat Shield at High Radiative Heating Rates

G. F. Greenwald* and V. A. Corea†
McDonnell Douglas Astronautics Company, Santa Monica, Calif.

Introduction

The present Thor booster configuration has three solid strap-on motors that burn during the first 40 sec of flight. The proposed addition of extra solid motors to the Thor booster (up to a total of nine motors in its most advanced configuration) increases the heating rates to the base region beyond the present capability of the insulation system to protect the many items of base hardware.

A testing program was initiated to screen several candidate materials of both ablative and insulative types to replace or augment the existing insulation system. One material, viz. a sandwich of quartz cloth and Fiberfrax felt, significantly outperformed all of the other materials tested.

Fig. 1 Installed heat shield.

Received July 16, 1969. This Note is based on work performed by the McDonnell Douglas Astronautics Company, Western Division, under NASA Contract NAS7-545. The authors are indebted to M. C. Coes, McDonnell Douglas Astronautics Company, Western Division, for her assistance in selecting the materials for the tests.

* Senior Engineer/Scientist, Delta Aero/Thermodynamics Section, Flight Mechanics Branch, Development Engineering, Western Division. Member AIAA.

† Engineer/Scientist Specialist, Delta Aero/Thermodynamics Section, Western Division.